Physics Letters B 711 (2012) 347–352

Contents lists available at SciVerse ScienceDirect

Physics Letters B

www.elsevier.com/locate/physletb

New structures in the continuum of ^{15}C populated by two-neutron transfer

F. Cappuzzello [a,b,*], C. Rea [c,d], A. Bonaccorso [c], M. Bondì [a,b], D. Carbone [a,b], M. Cavallaro [b], A. Cunsolo [b], A. Foti [a,e], S.E.A. Orrigo [f], M.R.D. Rodrigues [g], G. Taranto [a,b]

[a] *Dipartimento di Fisica e Astronomia, Università di Catania, Via S. Sofia 64, 95125 Catania, Italy*
[b] *INFN, Laboratori Nazionali del Sud, Via S. Sofia 62, 95125 Catania, Italy*
[c] *INFN, Sezione di Pisa, Largo Pontecorvo 3, 56127, Pisa, Italy*
[d] *Dipartimento di Fisica, Università di Pisa, Largo Pontecorvo 3, 56127 Pisa, Italy*
[e] *INFN, Sezione di Catania, Via S. Sofia 64, 95125 Catania, Italy*
[f] *Instituto de Física Corpuscular, CSIC, Universidad de Valencia, 46071 Valencia, Spain*
[g] *Instituto de Física, Universidade de São Paulo, C.P. 66318, 05315-970 São Paulo, SP, Brazil*

ARTICLE INFO

Article history:
Received 20 October 2011
Received in revised form 12 March 2012
Accepted 5 April 2012
Available online 13 April 2012
Editor: V. Metag

Keywords:
Transfer reactions
States of ^{15}C
Two-neutron break-up

ABSTRACT

The ^{13}C(^{18}O,^{16}O)^{15}C reaction has been studied at 84 MeV incident energy. The ejectiles have been detected at forward angles and ^{15}C excitation energy spectra have been obtained up to about 20 MeV. Several known bound and resonant states of ^{15}C have been identified together with two unknown structures at 10.5 MeV (FWHM = 2.5 MeV) and 13.6 MeV (FWHM = 2.5 MeV). Calculations based on the removal of two uncorrelated neutrons from the projectile describe a significant part of the continuum observed in the energy spectra. In particular the structure at 10.5 MeV is dominated by a resonance of ^{15}C near the ^{13}C + n + n threshold. Similar structures are found in nearby nuclei such as ^{14}C and ^{11}Be.

1. Introduction

Two-neutron transfer reactions are basic tools to explore neutron–neutron correlations inside the atomic nuclei [1]. They are essential to excite two-particle configurations built on a nucleus and reveal the features of the residual interactions, such as the pairing force, that are beyond the standard mean field description of nuclear structure. A massive literature has been constructed during the last decades on spectroscopic studies driven mainly by (p,t) or (t,p) reactions, accompanied by complementary studies with heavier projectiles [2]. Excellent reports about these latter topics are available, where the most advanced analyses are presented [3–5].

An important issue when dealing with two-neutron transfer reactions is that the direct one-step and the sequential two-step mechanisms contribute coherently to the observed cross section [5]. From a spectroscopic point of view, the former only allows the excitation of pair modes in the residual nucleus, where the two neutrons cluster together with an intrinsic angular momentum S orbiting around the core with an angular momentum L (L–S coupling). Sequential routes are, however, more effective in exciting configurations where each neutron independently couples with the core with an angular momentum j (j–j coupling). As a consequence, one should disentangle the direct and the sequential contributions in order to draw conclusions of spectroscopic interest.

Since many years it has been established that at bombarding energies not much above the Coulomb barrier, heavy-ion direct transfer reactions are valuable tools for getting precise spectroscopic information [3,4]. In this energy domain the reaction should be treated in a fully quantum-mechanical approach such as Distorted Wave Born Approximation (DWBA) or Coupled Channel Born Approximation (CCBA) [6], with the explicit inclusion of the nuclear recoils [4,7]. In such a framework it is possible to reproduce the observed L-dependent rapid oscillations of the angular distributions [8,9]. On the other hand semi-classical approaches have proved to be accurate enough to explain integral properties such as the selectivity of the reaction. As an example, matching conditions for the optimum linear and angular momentum transfer are known since many years [10], showing the crucial role of the incident energy and the reaction Q-value. An advantage of these semi-classical approaches is that the transfer to bound and unbound states can be treated in a coherent way. In Ref. [11] it has also been shown that different contributions to the reaction, such as elastic break-up and absorption from target bound states and resonances can be distinguished, at least for the case of one-neutron transfer.

* Corresponding author at: Dipartimento di Fisica e Astronomia, Università di Catania, Via S. Sofia 64, 95125 Catania, Italy.
E-mail address: cappuzzello@lns.infn.it (F. Cappuzzello).

0370-2693/$ – see front matter
http://dx.doi.org/10.1016/j.physletb.2012.04.012

An experimental program, aiming at the systematic investigation of two-particle excitations via the (^{18}O, ^{16}O) reaction, has been recently started at the INFN-LNS laboratories in Catania (Italy) using the MAGNEX spectrometer [12–15]. Such reactions are characterized by a high degree of selectivity for the excitation of two-particle configurations built over the target ground states [5,7,16,17]. The high resolution and large acceptance obtained in the detection of the ejectiles allow one to get high quality inclusive spectra, even in the largely unexplored region above the two-neutron emission threshold in the residual nucleus.

Nevertheless, the various components of projectile break-up in the energy spectra must be identified in order to isolate the spectral characteristics of the resonant-like excitations in the residue. An accurate and complete model of the two-neutron simultaneous-removal mechanism populating final continuum states is at present not available, mainly because of the difficulties of introducing a simple, but coherent, treatment of neutron–neutron correlations in the reaction dynamics. A recent attempt to develop such a model is found in Ref. [18].

In this Letter we report on the study of the ^{15}C continuum in which two unknown structures have been populated for the first time. The point of view of an independent removal of two neutrons successfully describes the ^{13}C(^{18}O, ^{16}O) reaction at 84 MeV.

2. The experiment

In the experiment a beam of $^{18}O^{6+}$ ions at 84 MeV incident energy, accelerated by the Tandem Van de Graaff, bombarded a 50 μg/cm^2 self-supporting 99% enriched ^{13}C target. A total beam charge of 110 ± 5 μC was integrated. The ^{16}O ejectiles were momentum analyzed by the MAGNEX spectrometer, working in full acceptance mode (solid angle $\Omega \sim 50$ msr and momentum range $\Delta p/p \sim 24\%$). In the measurements the spectrometer was set to cover an angular range between 7.5° and 17.5° in the laboratory reference frame. Supplementary runs with a 49 μg/cm^2 self-supporting ^{12}C target were recorded in order to estimate the background in the ^{16}O energy spectra from ^{12}C impurities in the ^{13}C target. A 120 μg/cm^2 self-supporting ^{9}Be target was also used for a short comparison run. The magnetic fields were set to accept oxygen ions with electric charge from 6^+ to 8^+. These were identified, event by event, by the simultaneous measurement of the position and angle at the focal plane, the energy loss in the gas sections of the focal plane detector and the residual energy on the silicon detector hodoscope [19]. Details about this technique are in Ref. [20].

The horizontal and vertical positions and angles of the identified ^{16}O ions, measured at the focal plane, are used as an input for a 10th order reconstruction of the scattering angle and momentum modulus, based on the fully algebraic method implemented in MAGNEX [21–26]. This allows an effective compensation of the high-order aberrations connected with the large acceptance of the spectrometer. The Q-values, or equivalently the excitation energies $E_x = Q_0 - Q$ (where Q_0 is the ground to ground state Q-value), are then obtained by the application of relativistic kinematic transformations. An overall energy and angular resolution of about 160 keV and 0.3° is obtained, mainly determined by the straggling introduced by the target. The total error in the measured absolute cross section is about 10%, induced by the uncertainty in the target thickness and beam collection.

3. Features of the energy spectra

Examples of the energy spectra measured at forward angles are shown in Figs. 1, 2 and 3. In the latter the contribution arising from the ^{12}C impurities in the target was found to be small and was subtracted, after normalization, from the final spectrum.

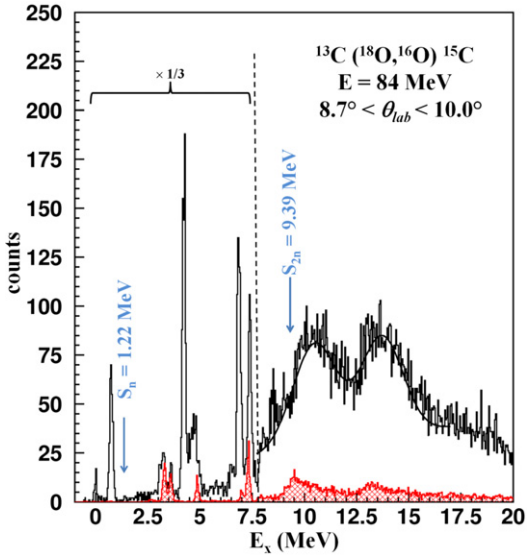

Fig. 1. Excitation energy spectrum of the ^{13}C(^{18}O, ^{16}O)^{15}C reaction at 84 MeV and $8.7° < \theta_{lab} < 10.0°$ (see text). The portion of the spectra on the left of the dashed line has been scaled by 1/3. A bin size of 42 keV is used and a resolution of 160 keV FWHM is obtained. The red hatched histogram represents the background arising from the ^{12}C(^{18}O, ^{16}O)^{14}C reaction coming from the ^{12}C impurity. The arrows at S_n and S_{2n} one- and two-neutron separation energies are drawn to guide the eye. The solid line superimposed to the histogram represents the result of the best fit discussed in the text. (For interpretation of the references to color in this figure, the reader is referred to the web version of this Letter.)

Two narrow states of ^{15}C are recognized in Fig. 1 below the one-neutron separation energy ($S_n = 1.218$ MeV), namely the ground and the only bound excited state at 0.74 MeV. Above the one-neutron separation threshold narrow states at excitation energy of $E_x = 3.10$, 4.22 4.66, 6.84, 7.35 MeV [27] are clearly identified. In addition, above the two-neutron emission threshold ($S_{2n} = 9.394$ MeV) two large unknown structures are strongly excited at energies $E_x = 10.5 \pm 0.1$ and 13.6 ± 0.1 MeV with Full Width at Half Maximum (FWHM) 2.5 ± 0.3 MeV for both. These are determined by best fit assuming Gaussian shapes and accounting for a three-body continuous background normalized to the region beyond 16 MeV. Other function shapes and background models were also used whose results are included in the error bars.

Seeking a clearer interpretation, the above inclusive spectrum can be divided into three regions bounded by S_n and S_{2n} in ^{15}C:

I. Between 0 and 1.218 MeV, where the ground and the first excited state at $E_x = 0.74$ MeV lie. A dominant $|\,^{15}C_{gs}(\frac{1}{2}^+)\rangle = |\,^{14}C_{gs}(0^+) \otimes (2s_{1/2})_\upsilon\rangle$ single particle configuration characterizes the ground and $|\,^{15}C_{0.74}(\frac{5}{2}^+)\rangle = |\,^{14}C_{gs}(0^+) \otimes (1d_{5/2})_\upsilon\rangle$ the excited state, both with a spectroscopic factor close to one [28,29]. In the past, these states have been customarily referred to as 1p–2h configurations on a ^{16}O 0^+ ground state core [27].

II. Between 1.218 and 9.394 MeV, where the continuum of the system $^{14}C + n$ mixes together with the negative parity quasi-bound states of the system $^{13}C + 2n$, typically labeled as 2p–3h configurations. These states are strongly excited by the (t, p) reaction reported by Truong and Fortune [27] where their complex nature of a p-shell neutron hole coupled with a two-neutron pair in the sd-shell was ascertained. In the present case the spectrum shows narrow peaks from the population of such 2p–3h states on the top of a continuous background whose shape arises from unbound non-resonant

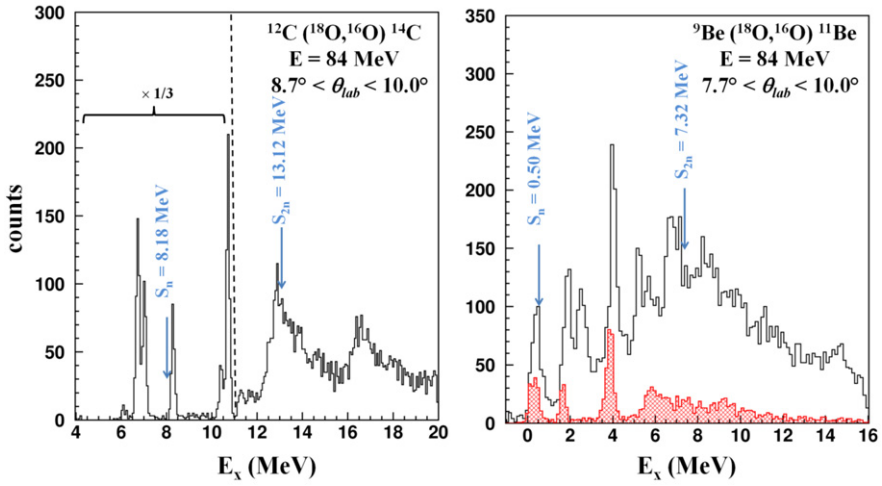

Fig. 2. Left panel: Excitation energy spectrum of the ^{12}C(^{18}O,^{16}O)^{14}C reaction at 84 MeV and 8.7° < θ_{lab} < 10.0°. The portion of the spectrum on the left of the dashed line has been scaled by 1/3. Right panel: Excitation energy spectrum of the ^{9}Be(^{18}O,^{16}O)^{11}Be reaction at 84 MeV and 7.7° < θ_{lab} < 10.0°. The red hatched histogram in the right panel represents the background due to the ^{12}C(^{18}O,^{16}O)^{14}C reaction coming from the ^{12}C impurity. In each histogram two arrows at S_n and S_{2n}, the one- and two-neutron separation energies, are drawn to guide the eye. (For interpretation of the references to color in this figure, the reader is referred to the web version of this Letter.)

^{14}C + n system phase space. The known narrow resonances with 1p–2h structure at 4.78, 5.81, 6.37, 6.43, 6.54, 7.10 MeV [30,31] and the Fano resonance at 8.50 MeV [32,33] are not observed or rather weakly populated, which is similar to measurements with (t, p) reactions.

III. Above 9.394 MeV, where the ^{13}C + 2n system is also unbound, a supplementary continuous distribution is expected from this channel. The narrow resonances with 3p–4h structure observed at 9.79, 10.25, 11.02, 11.83, 13.1, 13.8, 14.57, 16.0, 17.8 and 19.0 MeV in the ^{12}C(^{12}C,^{9}C)^{15}C [34,35] and partly in the ^{9}Be(^{7}Li,p)^{15}C [36] reactions are not observed or rather weakly populated.

A remarkably similar behavior is observed in the ^{11}Be and ^{14}C spectra shown in Fig. 2. In both cases narrow peaks are present up to the corresponding S_{2n} energy threshold and a sudden enhancement of the yield, fragmented in larger structures, is observed just above. The narrow peaks correspond to transitions to well-known excited states of ^{11}Be and ^{14}C, respectively, efficiently populated also by (t, p) reactions [37–39]. The similarity between the ^{14}C and ^{15}C spectra is even more evident in Fig. 1, where the ^{14}C spectrum is represented in the ^{15}C excitation energy parameter.

For the ^{14}C case, the states at 7.02 and 10.74 MeV, whose main configuration requires the coupling of two neutrons in the sd shell with the ^{12}C$_{gs}$(0$^+$) ground state core [38,40], are strongly populated. Near the S_{2n} threshold, the narrow states at 12.58, 12.89 and 12.96 MeV are superimposed to a large structure, steeply emerging at the threshold and slowing down up to about 16 MeV energy. A second unreported structure is also observed in the region between about 16 and 17.5 MeV.

Also in the ^{11}Be spectrum, the states at 3.96, 5.24 and 5.86, for which a ^{9}Be$_{gs}$ + 2n in the sd shells dominant configuration is reported [37], are among the most excited ones. In addition the structures observed above S_{2n} do not correspond to anything previously reported.

4. Theoretical description

The state of the art of the formalism of two-neutron transfer to bound states of the residual nucleus can be found in Ref. [5], where the theoretical aim was to obtain the inclusive angular distributions of the ejectiles. On the other hand, for transfer to the continuum, several angular momenta mix and the angular distributions are thus less useful. The energy distribution of the ejectile is the best observable to analyze in such cases. From it, the excitation energy spectrum of the residual nucleus is obtained by applying the energy conservation relation given in Ref. [11]. A complete description of the measured energy spectra would require a coherent treatment of both one- and two-particle configurations for the bound and unbound systems. Moreover, the cross section should be built as a coherent sum of the sequential plus the direct pair transfer contribution. The construction of such a model is a very ambitious task, but to our knowledge still beyond the present status of the theory. Indeed a calculation of a continuum extending from 0 to 20 MeV as we have done here for one of two neutrons would not be possible with DWBA nor with CCBA. In these cases an alternative approach could be the Coupled Channel Discretized Continuum. Nevertheless, to our knowledge this latter is still not stable, due to the huge computation requirements, when the high excitation energy region (above 8–10 MeV) is to be described, since the n–target wave-function is not well localized. Furthermore, these methods are able to deal with a neutron–target potential that only has a real part and is also energy independent. Here instead, we will show in the following that the absorption part is dominant in the region above the two-neutron threshold and that this can be obtained only with a complex neutron–target interaction.

Also in the case of purely independent two-neutron transfer to bound states, it is well known that, to the second order, the direct pair transfer amplitude cancels out with the non-orthogonal term of the sequential route [41].

Therefore, as a first step we made exploratory calculations on ^{15}C using a generalization of the one-nucleon transfer to unbound states model [11]. The method, in turn, extends the formalism of the transfer to bound states [42,43] to the case of unbound ones [44,45], assuming an uncorrelated removal of the two neutrons. What is left out is the specific treatment of nucleon–nucleon correlations beyond the ^{15}C mean field, as, for example, those due to the neutron–neutron pairing in the sd shells.

The reaction studied is then interpreted as a two-step mechanism: ^{18}O + ^{13}C → ^{17}O + ^{14}C$_{gs}$ → ^{16}O + ^{14}C$_{gs}$ + n starting from S_n; ^{18}O + ^{13}C → ^{17}O + ^{13}C$_{gs}$ + n → ^{16}O + ^{13}C$_{gs}$ + n + n starting from S_{2n}. This should account for a sizable component of the observed spectra. The justification relies on the fact that there is an almost perfect matching condition (consistent with Ref. [10]) between the single neutron separation energy of ^{18}O, S_n(^{18}O) = 8.044 MeV,

and the energy needed by the ^{13}C nucleus to get one neutron, i.e., the single neutron separation energy of ^{14}C: $S_n(^{14}\mathrm{C}) = 8.176$ MeV. Thus, in the first step of the reaction, the ground state to ground state Q-value is very small, $Q_0 = 0.132$ MeV, which implies an almost perfect match and thus a sudden process for the first neutron transfer, while the other neutron is transferred to the continuum of the ^{14}C system. For very low energies carried by the neutron, the ground and first bound excited state of ^{15}C are populated. For higher neutron energies, the resonances of ^{15}C are excited up to the $2n$ threshold energy. Crossing this threshold, the transfer to the continuum of $^{14}\mathrm{C} + n$ and the transfer to the continuum of $^{13}\mathrm{C} + n + n$, originated in the first step, merge together.

The cross section is given within a semi-classical model as an integration over the core–target distances of closest approach:

$$\frac{d\sigma_{1n}}{d\varepsilon_f} = C^2S \int_0^\infty b\,db \frac{dP(b)}{d\varepsilon_f} P_{el}(b) \tag{1}$$

and the total break-up cross section is obtained by integrating over the neutron final continuum energy ϵ_f, calculated with respect to the target. C^2S is the spectroscopic factor of the neutron single particle initial state. The factor $P_{el}(b) = |S_{cT}|^2 = \exp(-\ln 2 \exp[(R_s - b)/\Delta])$ is the core survival probability [46] in the elastic channel written in terms of the parameterized S-matrix for the core–target scattering. This is possible since the conditions for the semi-classical approximation to the relative ion–ion scattering apply to the reaction discussed in this work. We adopt the definition of the strong absorption radius, according to Ref. [47], as $R_s = 1.4(A_P^{1/3} + A_T^{1/3})$ in fm, which corresponds to the distance of closest approach for a trajectory that is 50% absorbed from the elastic channel. $\Delta = 0.6$ fm is a diffuseness-like parameter. This parameterization leads to reaction cross sections consistent with the Kox systematic [48]. Eq. (1) gives the final neutron energy distribution which is related by energy conservation to the measured ejectile energy distribution [45]. This model takes into account the fact that break-up reactions are sensitive only to the outermost tails of the single particle initial state wave functions which are taken as Hankel functions.

The transfer probability to final unbound states is

$$\frac{dP}{d\varepsilon_f} = \sum_{j_f} \left(|1 - \bar{S}_{j_f}|^2 + 1 - |\bar{S}_{j_f}|^2\right) \frac{e^{-2\eta b}}{\eta b} F(j_f, j_i) \tag{2}$$

where the form factor $\frac{e^{-2\eta b}}{\eta b}$ multiplies the $F(j_f, j_i)$ function, given in Ref. [45], which includes the kinematics and the angular momentum couplings. $\bar{S}_{j_f}$ is the energy-averaged (due to the continuum conditions) and angular-momentum dependent optical model S-matrix which describes the neutron–target interaction. The calculation of the S-matrix, strongly related to the choice of the neutron target optical potential, is an important point of this formalism. The first term in Eq. (2), proportional to $|1 - \bar{S}_{j_f}|^2$, gives the neutron elastic break-up or diffraction, while the second term proportional to $1 - |\bar{S}_{j_f}|^2$ gives the neutron absorption (or stripping) by the target.

Our calculations require the knowledge of both initial and final single-particle states of the transferred nucleon. For this reason, it is important to distinguish between bound and unbound states, since the potential used to describe them can be rather different, in particular for neutron-rich nuclei. In principle, the optical potential necessary to calculate the S-matrix that determines the final states in the continuum is energy dependent. In our case the final energy range sampled by the neutron in the continuum is less than 20 MeV. In this energy range, the optical potentials for neutron scattering on light nuclei are poorly known, because of the strong variation of the cross section characterized by very sharp resonances. Thus a constant potential from the parameterization given in Ref. [49] for $n + {}^{13}$C and $E = 10$ MeV has been adopted, after checking that an energy-dependent potential would only change the overall normalization within 30%. This has a Woods–Saxon real volume plus a spin–orbit and surface imaginary terms.

Table 1
Parameters for ^{17}O and ^{18}O bound state calculation.

	^{17}O ($1d_{5/2}$)	^{18}O ($1d_{5/2}$)
ϵ (MeV)	−4.143	−8.044
V_0 (MeV)	−62.7	−68.1
C_i (fm$^{-1/2}$)	0.69	1.34

The radial wave functions of the initial (projectile) bound states have been obtained as numerical solution of the Schrödinger equation with depths V_0 of the Woods–Saxon potentials adjusted to reproduce the experimental separation energies ϵ. In particular, a radius of 2.91 fm and diffuseness of 0.56 fm were used for the central potential and depth of 5.5 MeV, radius of 2.96 fm and diffuseness of 0.5 fm for the spin orbit term. The results are given in Table 1. From the bound states wave functions we have then obtained the asymptotic normalization constants C_i of the single particle states. It is interesting to note that the asymptotic normalization constants in Table 1 are consistent with those used in Ref. [50] in a recent calculation of reactions rates of astrophysical interest involving the same oxygen and carbon nuclei studied here.

5. Data analysis

The continuum spectrum of ^{15}C is given in Fig. 3 where the data are plotted together with results obtained using the approach described above. Between S_n and S_{2n} the calculation, given by the red dashed curve, contains the three-body physical background due to the elastic break-up only, as given by the first term of Eq. (2). In this region, in fact, the absorption observed in the data is dominated by the narrow (2p–3h) resonances stabilized by n–n pairing, which is not accounted for in our approach. The knowledge of a correct energy and angular momentum dependence of the n–n pair + core optical potential would be necessary to give a precise description of such resonances. This could be achieved only with a microscopically calculated optical potential, which is still an unresolved problem. Therefore a description of the absorption based on the optical model is not feasible in this region. On the other hand, above the S_{2n} threshold the resonances are quite smooth and we calculated there both elastic (red double-dashed-dotted curve) and absorption (green dotted curve) terms. The dashed-dotted orange curve is their sum. Finally, the violet full curve is the sum of all contributions in the two regions considered, folded with the experimental resolution. All calculations include a spectroscopic factor of 0.8 for the initial state, according to Ref. [51].

The structure at 10.5 MeV in the experimental spectrum is reproduced in the calculation as a convolution of the peak calculated in the $^{13}\mathrm{C} + n + n$ channel and the tail of the $^{14}\mathrm{C} + n$ elastic break-up. The main contribution comes from the absorption of the two neutrons. This means that a $^{13}\mathrm{C} + n + n$ resonant configuration can account for the observed structure, without the need of introducing specific n–n correlations.

Since Eq. (2) contains an incoherent sum over final angular momenta, it allows an estimate of the contribution of each single l value to the total sum. This can help to understand the origin of the strength distribution in the spectrum. In Fig. 4 the calculations

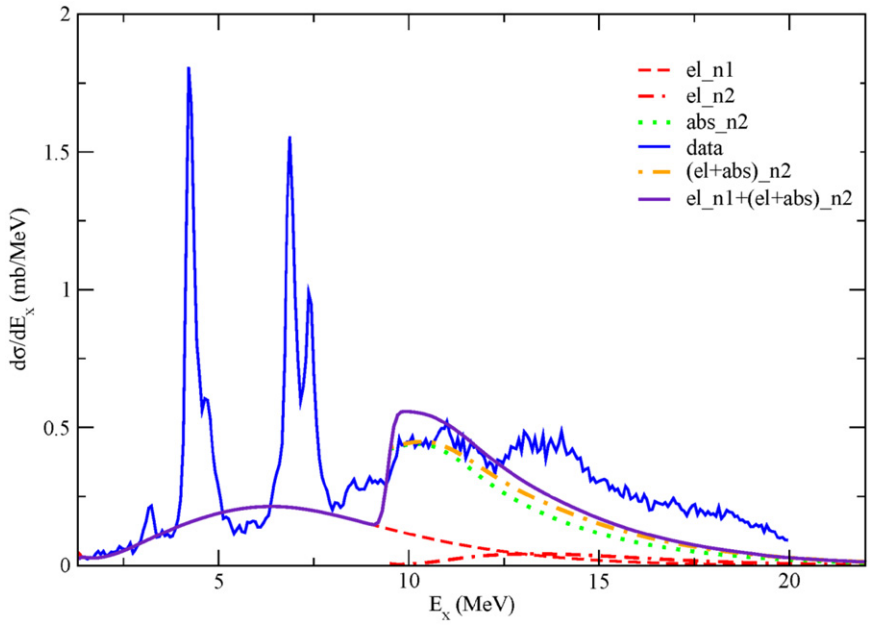

Fig. 3. Inclusive energy spectrum of the reaction for $7.5° < \theta_{lab} < 17.5°$ and theoretical calculations of various break-up components (see text). The red dashed (el_n1) and red double-dashed-dotted (el_n2) curves represent the one- and two-neutron elastic break-up, respectively. The green dotted curve (abs_n2) represents the two-neutron absorption term. The orange dashed-dotted curve ((el+abs)_n2) is the sum of two-neutron elastic break-up and absorption. Finally, the violet full curve ((el_n1+(el+abs)_n2) is the sum of all contributions folded with the experimental resolution. In the experimental spectrum, plotted with a bin size of 70 keV, the background from the ^{12}C impurity has been subtracted (see Fig. 1). (For interpretation of the references to color in this figure legend, the reader is referred to the web version of this Letter.)

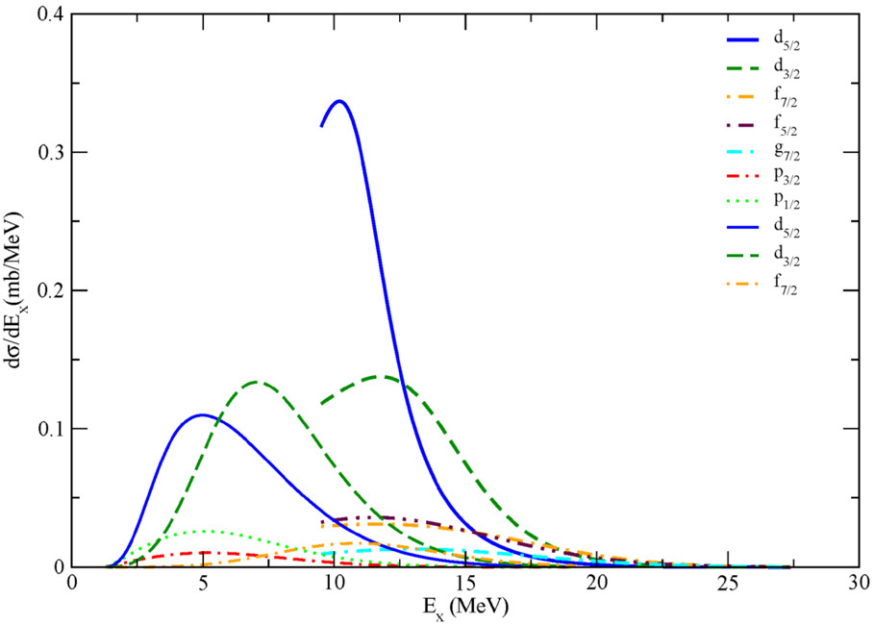

Fig. 4. Dominant contributions to the partial wave decomposition of the theoretical energy spectrum shown in Fig. 3. The legend indicates the single particle angular momentum of each individual strength distribution. The lines starting at $E_x = 1.218$ MeV refer to the $^{14}C + n$ system while those starting at 9.394 MeV to the $^{13}C + n + n$ (see text).

between S_n and S_{2n} represent the partial wave decomposition of the n–^{14}C elastic break-up cross section. One can see that the main contribution in this region comes from the $d_{5/2}$ and the $d_{3/2}$ states, a result that is consistent with the literature [48]. It also appears from Fig. 4 that above S_{2n} the main source of cross section comes from configurations where both neutrons are transferred to the $d_{5/2}$ and $d_{3/2}$ continuum orbitals. The combination gives also a good account of the background at higher excitation energy, but does not reproduce the bump at 13.6 MeV. This indicates that a more complete description of the $^{13}C + n + n$ system, including the n–n correlations is required here. Similarly to that observed between S_n and S_{2n} the existence of $(^{13}C + n)$–n pair resonances could act in redistributing and/or adding further strength beyond the S_{2n} threshold.

6. Conclusions

In this Letter we have reported the results of the $(^{18}O, ^{16}O)$ reaction on ^{13}C, ^{12}C and ^{9}Be targets at 84 MeV incident energy. The effects of the two-neutron transfer from the projectile, pop-

ulating a large region of the continuum of the target plus two-neutron system, have been studied by measuring the missing mass of ^{16}O and interpreted for the first time. Below the S_{2n} threshold, in the corresponding residual nucleus spectrum, the cross section is mainly concentrated in the bound states and in a number of known sharp resonances emerging above a rather small flat continuous background. A sudden increase of the measured ^{16}O yield is observed starting from the S_{2n} threshold, appearing in the shape of previously unobserved large bumps. In the case of ^{15}C these are centered at 10.5 MeV (FWHM $\sim$ 2.5 MeV) and 13.6 MeV (FWHM $\sim$ 2.5 MeV). We note that the states with a known 2p–3h structure exhaust a consistent amount of the measured cross section, with negligible contribution from states with a known 1p–2h, namely the two bound states, or 3p–4h configuration. This indicates the fundamental role of the n–n correlations in these experimental conditions.

Both the elastic break-up and absorption channels have been analyzed in a consistent way for the ^{13}C(^{18}O, ^{16}O)^{15}C reaction. In the adopted theoretical model, the scattering of the neutrons independently removed from the projectile as it passes the target nucleus is described by means of an optical potential with a semi-classical approximation for the relative motion. The absolute value of the theoretical cross section might vary, within 30%, depending on the details of the potential. Instead, the calculated shapes of the spectra are almost independent on this, and in all cases the calculations show that the elastic break-up represents a minor part of the continuous spectra, which are in fact dominated by the absorption of both neutrons. In particular, the bump at 10.5 MeV is described in terms of an enhanced probability, near the S_{2n} threshold, of exciting $^{13}\mathrm{C} + n + n$ configurations where the two neutrons are mainly transferred to $d_{5/2}$ or $d_{3/2}$ resonances of the resulting ^{15}C nucleus. Also, the average behavior of the spectrum at higher energies is reasonably well described within the assumption of the independent transfer of neutrons. The model cannot account for the strong population of narrow resonances with known 2p–3h configuration observed between S_n and S_{2n}, because of the lack of n–n correlations. Also, the bump at 13.6 MeV is missed, which could indicate a similar structure for all these states. An explicit treatment of the full $^{13}\mathrm{C} + n + n$ interaction, including the n–n pairing, would be required to understand the remaining details of the energy spectra. Preliminary theoretical investigation of the (^{18}O, ^{16}O) reaction data on ^{12}C and ^{9}Be, along the same lines discussed in this Letter, confirm our interpretation of the large structures, namely the combined effects of the two neutrons in continuum states of low angular momentum. The study of the angular distributions and of the decaying products for the systems studied in this Letter, as well as for similar cases, should allow one to shed more light on the role of such n–n correlations.

Acknowledgements

We should like to thank Dr. J.S. Winfield for his critical reading of the manuscript.

References

[1] D.R. Bes, R.A. Sorensen, in: M. Baranger, E. Vogt (Eds.), The Pairing-Plus-Quadrupole Model, in: Advances in Nuclear Physics, vol. 2, Plenum Press, New York, 1969, pp. 129–222.
[2] R.A. Broglia, O. Hansen, C. Riedel, in: M. Baranger, E. Vogt (Eds.), Two-Neutron Transfer Reactions and the Pairing Model, in: Advances in Nuclear Physics, vol. 6, Plenum Press, New York, 1973, pp. 287–457.
[3] N. Anyas-Weiss, et al., Phys. Rep. 12 (1974) 201.
[4] S. Kahana, A.J. Baltz, in: M. Baranger, E. Vogt (Eds.), One- and Two-Neutron Transfer Reactions with Heavy Ions, in: Advances in Nuclear Physics, vol. 9, Plenum Press, New York, 1977, pp. 1–122.
[5] W. von Oertzen, A. Vitturi, Rep. Prog. Phys. 64 (2001) 1247, and references therein.
[6] G.R. Satchler, Direct Nuclear Reactions, Oxford Science Publications, 1983.
[7] M.C. Mermaz, et al., Phys. Rev. C 20 (1979) 2130.
[8] D. Sinclair, Phys. Lett. B 53 (1974) 54.
[9] M.J. LeVine, et al., Phys Rev. C 10 (1974) 1602.
[10] D.M. Brink, Phys. Lett. B 40 (1972) 37.
[11] A. Bonaccorso, I. Lhenry, T. Soumijärvi, Phys. Rev. C 49 (1994) 329.
[12] F. Cappuzzello, et al., in: Magnets: Types, Uses and Safety, Nova Publisher Inc., New York, 2011, pp. 1–63.
[13] A. Cunsolo, et al., Nucl. Instr. Methods A 481 (2002) 48.
[14] A. Cunsolo, et al., Eur. Phys. J. Spec. Topics 150 (2007) 343.
[15] M. Cavallaro, et al., AIP Conf. Proc. 1213 (2009) 198.
[16] M. Cavallaro, et al., J. Phys.: Conf. Series 312 (2011) 092020.
[17] D. Carbone, et al., J. Phys.: Conf. Series 312 (2011) 082016.
[18] M. Assié, D. Lacroix, Phys. Rev. Lett. 102 (2009) 202501.
[19] C. Boiano, et al., IEEE Trans. Nucl. Sci. 55 (2008) 3563.
[20] F. Cappuzzello, et al., Nucl. Instr. Methods A 621 (2010) 419.
[21] F. Cappuzzello, et al., Nucl. Instr. Methods A 638 (2011) 74.
[22] M. Cavallaro, et al., Nucl. Instr. Methods A 637 (2011) 77.
[23] A. Lazzaro, et al., Nucl. Instr. Methods A 570 (2007) 192.
[24] A. Lazzaro, et al., Nucl. Instr. Methods A 585 (2008) 136.
[25] A. Lazzaro, et al., Nucl. Instr. Methods A 591 (2008) 394.
[26] A. Lazzaro, et al., Nucl. Instr. Methods A 602 (2009) 494.
[27] S. Truong, Phys. Rev. C 28 (1983) 977.
[28] G. Murillo, S. Sen, S.E. Darden, Nucl. Phys. A 579 (1994) 125.
[29] J.R. Terry, et al., Phys. Rev. C 69 (2004) 054306.
[30] J.D. Goss, et al., Phys. Rev. C 8 (1973) 514.
[31] S.E. Darden, G. Murillo, S. Sen, Phys. Rev. C 32 (1985) 1764.
[32] F. Cappuzzello, et al., Europhys. Lett. 65 (2004) 766.
[33] S.E.A. Orrigo, et al., Phys. Lett. B 633 (2006) 469.
[34] H.G. Bohlen, et al., Phys. Rev. C 68 (2003) 054606.
[35] H.G. Bohlen, et al., Eur. Phys. J. A 31 (2007) 279.
[36] J.D. Garrett, F. Ajzenberg-Selove, H.G. Bingham, Phys. Rev. C 10 (1974) 1730.
[37] G.B. Liu, H.T. Fortune, Phys. Rev. C 42 (1990) 167.
[38] S. Mordechai, et al., Nucl. Phys. A 301 (1978) 463.
[39] F. Ajzenberg-Selove, E.R. Flynn, O. Hansen, Phys. Rev. C 17 (1978) 1283.
[40] W. Von Oertzen, et al., Eur. Phys. J. A 21 (2004) 193.
[41] R.A. Broglia, A. Winther, Heavy Ion Reactions: The Elementary Precessess, Addison-Wesley, Reading, MA, 1991, p. 306.
[42] L. Lo Monaco, D.M. Brink, J. Phys. G 11 (1985) 935.
[43] A. Bonaccorso, D.M. Brink, L. Lo Monaco, J. Phys. G 13 (1987) 1407.
[44] A. Bonaccorso, D.M. Brink, Phys. Rev. C 38 (1988) 1776.
[45] A. Bonaccorso, D.M. Brink, Phys. Rev. C 43 (1991) 299.
[46] A. Bonaccorso, Phys. Rev. C 60 (1999) 054604.
[47] D.M. Brink, Semi-Classical Methods for Nucleus–Nucleus Scattering, Cambridge University Press, 1986.
[48] S. Kox, et al., Phys. Rev. C 35 (1987) 1678.
[49] J.H. Dave, C.R. Gould, Phys. Rev. C 28 (1983) 2212.
[50] J.T. Huang, C.A. Bertulani, V. Guimarães, Atomic Data and Nuclear Data Tables 96 (2010) 824.
[51] S. Burzynski, et al., Nucl. Phys. A 399 (1983) 230.